## Related topics
Magnetic moment, Bohr magneton, directional quantization, g-factor, electron spin, atomic beam, Maxwell velocity distribution, two-wire field.

## Principle
A beam of potassium atoms generated in a hot furnace travels along a specific path in a magnetic field, which corresponds to a two-wire field. Because of the spin magnetic moment of the potassium atoms, the gradient of the inhomogeneous field produces a force, ortogonal to the direction of motion. The potassium atoms are thereby deflected from the straight ballistic trajectory according to their spin quantization. By measuring the density of the beam of particles in a plane of detection behind the magnetic field area it is possible to draw conclusions to the magnitude and direction of their magnetic moment.

Fig 1: Experimental setup; Stern-Gerlach apparatus with high vacuum pump assembly.

  

## Equipment

| | | |
|---|---|---|
| 1 | Stern-Gerlach apparatus | 09054-88 |
| 1 | Matching transformer | 09054-04 |
| 1 | Potassium ampoules, set of 6 | 09054-05 |
| 1 | High vacuum pump assembly, compact | 09059-99 |
| 1 | Electromagnet w/o pole shoes | 06480-01 |
| 2 | Pole piece, plane | 06480-02 |
| 1 | Commutator switch | 06034-03 |
| 2 | Voltmeter, 0.3-300 VDC, 10-300 VAC | 07035-00 |
| 2 | Ammeter, 1 mA – 3 A DC/AC | 07036-00 |
| 1 | Meter, 10/30 mV, 200 °C | 07019-00 |
| 1 | Storage tray 413x240x100mm | 47325-02 |
| 1 | Cristallising dish, boro 3.3, 2300 ml | 46246-00 |
| 1 | Isopropyl alcohol, 1000 ml | 30092-70 |
| 1 | DC measuring amplifier | 13620-93 |
| 1 | Power supply variable 15 VAC/ 12 VDC/ 5 A | 13530-93 |
| 2 | Power supply 0-12 V DC/ 6 V, 12 V AC, 230 V | 13506-93 |
| 1 | Two-tier platform support | 02076-03 |
| 3 | Rubber tubing, vacuum, i.d. 6 mm | 39286-00 |
| 2 | Connecting cord, *l* = 250 mm, yellow | 07360-02 |
| 2 | Connecting cord, *l* = 250 mm, blue | 07360-04 |
| 3 | Connecting cord, *l* = 500 mm, red | 07361-01 |
| 2 | Connecting cord, *l* = 500 mm, blue | 07361-04 |
| 1 | Connecting cord, *l* = 500 mm, green-yellow | 07361-15 |
| 1 | Connecting cord, *l* = 750 mm, red | 07362-01 |
| 3 | Connecting cord, *l* = 750 mm, yellow | 07362-02 |
| 1 | Steel cylinder, nitrogen, 10 l, full | 41763-00 |
| 1 | Reducing valve for nitrogen | 33483-00 |
| 1 | Gas-cylinder Trolley for 10 L. | 41790-10 |

## Tasks

1. Recording the distribution of the particle beam density in the detection plane in the absence of the magnetic field.
2. Fitting a curve consisting of a straight line, a parabola, and another straight line, to the experimentally determined spatial distribution of the particle beam density.
3. Observing the splitting of the particle beam in the magnetic field according to the spin quantization. Determining the dependence of the particle beam density in the detection plane on different values of the magnetic field gradient.
4. Investigating the positions of the maxima of the particle beam density as a function of the magnetic field gradient. Calculation of the Bohr magneton.

## Setup and procedure

In order to properly use the setup please first get through this experimental script and also the **manual to the Stern-Gerlach (09054-88) apparatus**.

### 1. Preparation of the vacuum system: evacuation

Prior to running the vacuum pump assembly please thoroughly read the supplied manuals from the manufacturer. Please note that the exact model of the pump assembly is the subject to be changed without notice. The pump stand consists of a rotary backing pump and a high vacuum turbo pump system controlled by a microprocessor. The nitrogen bottle should be connected through the proper tubing to the venting valve of the pump stand. Generally the system should be vented with nitrogen only. Venting with the atmospheric air leads to the moisture absorption inside the apparatus and thus to extreme long pump times (more than 24 hours to reach $5*10^{-6}$ mbar). This would also lead to potassium oxidation and thus degradation of the setup functionality. Venting of the hot potassium with air is strictly forbidden due to its following vigorous burning in oxygen. Generally it is recommended for the user to get acquainted with and program the controller according to the desired venting regime (e.g. its disabling during a student practicum). Furthermore the proper gas type regime of the turbo pump should be selected to optimize its efficiency and lifetime. It is generally discriminated between light gases (hydrogen, helium), medium gases, as in the present experiment, (nitrogen, oxygen) and heavy ones (xenon). The display of the controller should be routinely used to show the pressure inside the system. Time after time, but especially by the first start of the pumps, it is necessary to activate the purging valve of the rotary pump for a couple of hours to remove the water vapors or impurities, accumulated in the system.

**2. Preparation of the vacuum installation: filling**
Set the pressure reducer valve of the nitrogen gas bottle to the value below 500 hPa. Open the valves on the bottle and the pressure reducer. Activate venting from the pump assembly controller. Nitrogen flows in.

**3. Assembly of the Stern-Gerlach apparatus**
Remove the clamp from the blind vacuum flange on the oven but leave it on its place whereas the apparatus is positioned horizontally. Generally vacuum systems are not designed to sustain over-pressure, which can be easily prevented with this trick. It is recommended to use the system continuously without the clamp mentioned above. Under vacuum the atmospheric pressure creates sufficient force (roughly 100 N) to keep the vacuum connection sealed. During venting the blind flange will let the redundant nitrogen to escape by vibrating there and back and thus preventing over-pressure. Now remove the blind flange at the bottom of the setup, then quickly connect and clamp it to the pumping stand while nitrogen continuously flows through the system.

The electromagnet should be situated on its base support and the vacuum setup clamped between its coils. Make sure that its pole shoes are perfectly aligned relative to the Stern-Gerlach pole pieces and consequently clamp it without any gap or tilt – this is absolutely important to conduct the magnetic flux properly. To achieve that, sometimes it is necessary to untighten several of the vacuum flange clamps of the Stern-Gerlach apparatus and adjust the rotational orientation of the system. After that the installation is complete, please stop venting and evacuate the apparatus.

The system should reach a pre-vacuum level (ca. $10^{-2}$ mbar) in less than a couple of minutes. If it fails to do that, there should be a larger vacuum leak present – please stop pumping immediately in order not to overload the vacuum pumps and try to fix it. In several hours the system should reach the desired high vacuum level of approximately $5*10^{-6}$ mbar or less. Please note that it is not possible to work with the setup at worse vacuum level since collisions of K atoms with air molecules cannot be then neglected. If the specified above vacuum level cannot be achieved, all flanges should be checked for smaller leaks by dripping alcohol (e.g. isopropanol) on the connection peaces and observing the vacuum level. Any slight pressure change indicates such a small leak. The system should be vented with nitrogen and the problematic connection cleaned from dust, inspected for damages and reassembled very thoroughly.

**4. Charging the atomic beam furnace**
Make sure that the clamp of the blind flange of the potassium oven has been removed and vent the system with nitrogen. Do not stop nitrogen venting by loading of potassium to prevent its contact with the air oxygen. Remove the blind flange and also discard the safe transportation plastic cylinder from the furnace, insert the key for releasing the furnace threaded cap and turn to remove it. Then replace the blind flange back. Place a potassium ampule with its tip upwards into the steel cylinder of the ampule opener and cover it with its associated steel disc. Strike the steel disc with a hammer, thus cutting off the

  

top of the ampule as shown in Fig. 2. Caution should be taken when handling potassium! Contact with the skin causes burns. Wear protective goggles and gloves! After the use, throw any parts which have been in contact with potassium into a vessel containing isopropanol (vigorous reaction is possible). The potassium injector must be pushed as quickly as possible in the opened ampule as far as it will go in order to grasp the potassium completely. Withdraw the injector, strip off glass debris with a spatula, remove the blank flange from the atomic beam furnace, hold the injector inside the furnace, push out the potassium (using the injector like an ordinary syringe). Try to stick the clump of potassium to the back wall of the oven in order not to block the output atomic beam aperture on its front. Reinsert the furnace threaded cap and the blind flange. Stop venting and evacuate the setup to the high vacuum. Warm the oven up to the temperature of around 120° during an hour in order to degas it. After charging do not let any atmospheric air to come into the contact with oven, keep it always in vacuum or in nitrogen atmosphere till the new loading of potassium after some longer time period. After many working days the complete removal and cleaning of the furnace with isopropanol and subsequent drying in a laboratory oven can be considered before a fresh portion of potassium will be introduced.

Fig. 2: Breaking the glass ampule in order to load potassium into the furnace.

  

## 5. Electric circuit assembly

The electrical circuit is shown in Fig.3. To carry out a measurement without field it is recommended first to demagnetize the pole shoes of the electromagnet. This is done by reducing the coil current in steps by small amounts, reversing the polarity at each step using the commutation switch.

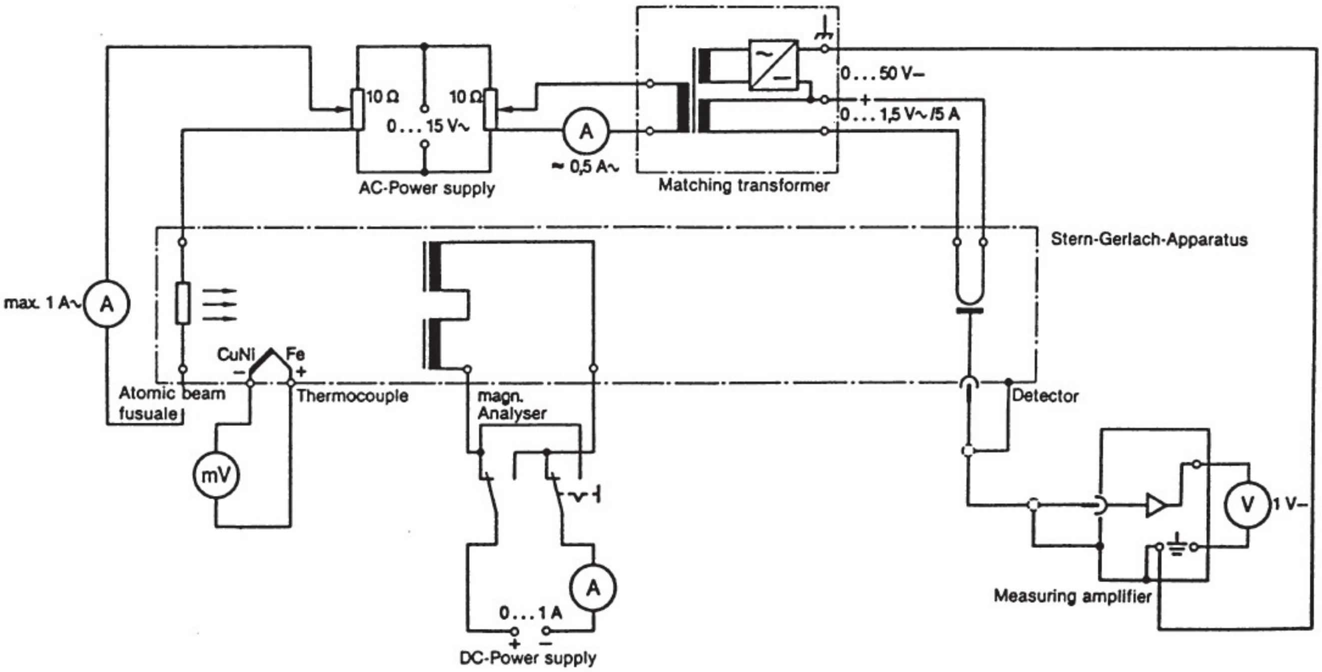


Fig. 3: Electrical circuit of the Stern-Gerlach experiment

## 6. Conduction of the experiment

When carrying out an experiment, make sure that the voltages applied to the atomic beam furnace and the matching transformer correspond to those given in the supplied with the experiment data sheet. The voltage on the Langmuir-Taylor detector should be optimized for each detector individually. A too low voltage will lead to the slow or no reaction (ionization) on the atomic beam. A too high voltage will provide additional undesirable dark current. Check the furnace heating voltage. Make sure that the thermocouple is plugged into the proper connectors of the analog multimeter for direct indication of the temperature on its display. (Wrong connection will lead to a low read out and thus overheating of the furnace.) When making a series of measurements by changing the position of the detector always turn the micrometer screw in one direction only to avoid the effect of mechanical hysteresis. Conduct measurements only after reaching stationary conditions (every electrical parameter and the temperature remain constant). The geometry of the apparatus required for evaluation is likewise specified in the data sheet and its manual.

## Theory and evaluation

## 1. Magnetic moment

A potassium atom has one outer shell electron in the ground state denoted $4s^1$. In this respect it is similar to silver atoms ($5s^1$ electron) which were used originally by Otto Stern and Walther Gerlach. The orbital angular momentum is equal to zero. The magnetic moment $\vec{\mu}$ of the potassium atom due to this outer electron is therefore attributable only to its spin S.

$$\vec{\mu} = -\frac{e}{2m_0} g_s \cdot \vec{S} \quad (1)$$

If one considers the component $S_z$ of the spin in a given *z*-direction, the system has two different possible orientations, characterized by the quantum numbers

$$m_s = \pm \frac{1}{2}$$

The *z*-component of spin takes the eigen value

$$S_z = m_s \hbar = \pm \frac{1}{2} \hbar$$

The associated magnetic moment in the z-direction takes the value

$$\mu_z = -\frac{e\hbar}{2m_0} m = -\mu_B m$$

with the Bohr magneton

$$\mu_B = \frac{e\hbar}{2m_0} = 9.274 \cdot 10^{-24} A m^2$$

and

$$m = m_s \cdot g_s$$

The literature value of the g-factor is

$$g_s \approx 2.0023 \quad (2)$$

Hence,

$$m = \pm 1.0012 \approx \pm 1 \quad (3)$$

The purpose of the Stern-Gerlach experiment is to observe the directional quantization of the electron spin. Furthermore, according to which quantity is taken as known, the value of $\mu_z ; \mu_B ; m$ or $g_s$ can be determined.

Let the direction of the magnetic field with field strength $\vec{H}$ and induction $\vec{B}$ entered by the potassium atoms be taken as *z*-coordinate. The outer electrons of the potassium atom complete a classical precession movement about the field direction. The eigen values of the magnetic moment are therefore parallel or anti-parallel to the magnetic field:

$$\vec{\mu}_H = \mu_z \frac{\vec{H}}{H} = -m \mu_B \frac{\vec{H}}{H} \quad (4)$$

**2. Action of forces**

The forces acting on the potassium atom are attributable to its magnetic moment and arise when the field is inhomogeneous:

$$\vec{F} = (\vec{\mu}_H \overrightarrow{grad}) \vec{B} = \mu_0 (\vec{\mu}_H \overrightarrow{grad}) \vec{H}$$

  

The expression in parentheses is to be understood as a scalar product whose differential operators act on $\vec{B}$ or $\vec{H}$ . The force is therefore determined by the gradient of the magnetic field:

$$\vec{F} = \mu_0 \mu_H \left( \frac{\vec{H}}{H} \overrightarrow{grad} \right) \vec{H}$$

We simplify this equation using the following equality

$$\frac{1}{2} grad\, H^2 = \left( \vec{H}\, \overrightarrow{grad} \right) \vec{H} + \vec{H}\, x\, \overrightarrow{curl}\, \vec{H}$$

in which the vector product of $\vec{H}$ and $\overrightarrow{curl}\, \vec{H}$ vanishes since

$$\overrightarrow{curl}\, \vec{H} = 0$$

Further, we can put

$$\frac{1}{2} \overrightarrow{grad}\, \vec{H}^2 = \frac{1}{2} \overrightarrow{grad}\, H^2 = H\, \overrightarrow{grad}\, H$$

i.e., only the scalar values *H* of the magnetic field are implied:

$$\vec{F} = \mu_0 \mu_H\, \overrightarrow{grad}\, H = \mu_H\, \overrightarrow{grad}\, B$$

For example, when using a Cartesian system of coordinates (x, y, z), the component of the force acting on the potassium atom in the z-direction equals

$$F_z = \mu_H \frac{\partial B}{\partial z}$$

or

$$F_z = -\, m \mu_B \frac{\partial B}{\partial z} \quad (5)$$

Assuming that the potassium atoms enter the magnetic field at right angles to it and leave it again after a path *Δl*, and that $\partial B / \partial z$ is constant, the potassium atoms describe a parabolic path and are deflected more or less strongly in the *z*-direction according to their different velocities of entry, with corresponding changes in direction.

The position of the plane *z* = 0 in the magnetic field must still be determined accurately.

### 3. Two-wire field

The pole shoes of a special shape can reliably simulate the magnetic field of two wires with electrical current in opposite directions as shown in Fig. 4. Their shape is plane-cylindrical and the outlines correspond to the two equipotential lines of the above-mentioned field.

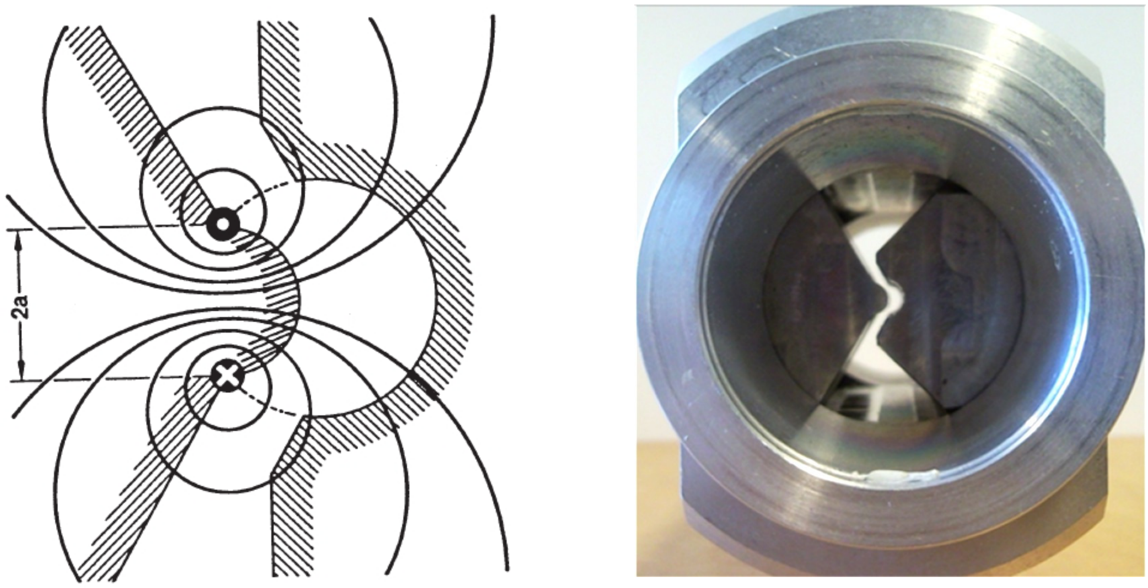


Fig. 4: Two-wire field simulation with special pole shoes.

The magnetization of the pole shoes should not reach saturation. In the treatment of the experimental problem with the two-wire model: The magnetic field $\vec{H}$ at some arbitrary point of space consists of the two components, $\vec{H}_1$ and $\vec{H}_2$ as shown in Fig. 5. $\vec{H}(\vec{r})=\vec{H}_1(\vec{r})+\vec{H}_2(\vec{r})$

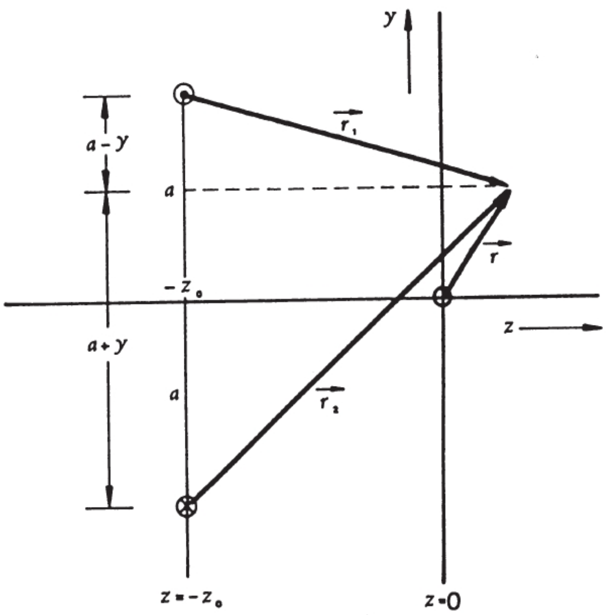


Fig. 5: Determination of a system of coordinates; the two-wire field model.

Each of the two conductors contributes to the field as follows:

$$\vec{H}_i(\vec{r}_i)=\frac{\vec{I}_i\times\vec{r}_i}{2\pi r_i^2},(i=1,2)$$

where

$$\vec{I}_1=-\vec{I}_2=\vec{I}$$

is the vector current in a single wire. Hence, for the arbitrary space point, specified by a vector $\vec{r}$ we can write down:

$$\vec{H}(\vec{r})=\frac{1}{2\pi}\vec{I}\times\left(\frac{\vec{r}_1}{r_1^2}-\frac{\vec{r}_2}{r_2^2}\right)$$

The value of the magnetic field strength is obtained by squaring this expression.

$$H^2(\vec{r})=\frac{I^2}{(2\pi)^2}\left(\frac{\vec{r}_1}{r_1^2}-\frac{\vec{r}_2}{r_2^2}\right)\left(\frac{\vec{r}_1}{r_1^2}-\frac{\vec{r}_2}{r_2^2}\right)=\frac{I^2}{(2\pi)^2}\left(\frac{1}{r_1^2}+\frac{1}{r_2^2}-\frac{2\vec{r}_1\vec{r}_2}{r_1^2r_2^2}\right)=\frac{I^2}{(2\pi)^2}\left(\frac{1}{r_1^2}+\frac{1}{r_2^2}+\frac{(\vec{r}_1-\vec{r}_2)^2-r_1^2-r_2^2}{r_1^2r_2^2}\right)$$

The vectors $\vec{r}_1$ and $\vec{r}_2$ are perpendicular to the vector $\vec{I}$ and $(\vec{r}_1-\vec{r}_2)^2=4a^2$ thus:

$$H(\vec{r})=\frac{I}{\pi}\frac{a}{r_1r_2} \quad (6)$$

The gradient of the magnetic field *H* as a function of z can be calculated, using the expressions

$$r_1^2=(a-y)^2+(z+z_0)^2$$

and

$$r_2^2=(a+y)^2+(z+z_0)^2$$

as

$$\frac{\partial H}{\partial z}=-\frac{Ia(z+z_0)}{\pi}\cdot\frac{(r_1^2+r_2^2)}{r_1^3r_2^3}=-\frac{2Ia(z+z_0)}{\pi}\cdot\frac{a^2+y^2+(z+z_0)^2}{((a^2-y^2)^2+2(z+z_0)^2\cdot(a^2+y^2)+(z+z_0)^4)^{3/2}} \quad (7)$$

The surfaces of the constant field gradient $\partial H/\partial z$ are shown in Fig. 6; on them also the force exerted onto a neutral potassium atom will be constant. The constant force surfaces in the neighborhood of the coordinate $z = z_1$, which we want to calculate, are flat in a good approximation.

In other words, we are looking for the plane $z = z_1$, in which the field gradient is approximately constant and calculating its position relative to the plane with the wires, $(z_0+z_1)=?$ . The gradient $\partial H/\partial z$ should be here independent of *y* for small *y*. Mathematically speaking, we develop the $\partial H/\partial z$ into a Taylor polynomial in the variable $y^2$ and look at which *z*-coordinate its first order term will be equal to zero.



  

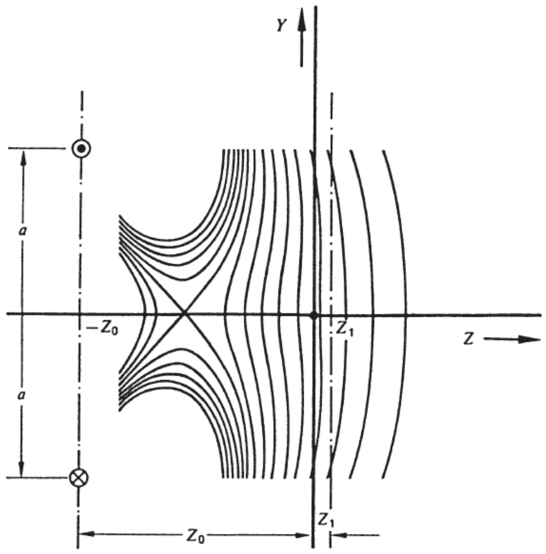


Fig. 6: Lines of the constant field gradient $\frac{\partial H}{\partial z}$ .

$$\frac{\partial H}{\partial z}(z=z_1) \approx -\frac{2Ia(z_0+z_1)}{\pi(a^2+(z+z_1)^2)^2}\cdot\left(1+\frac{2a^2-(z+z_1)^2}{(a^2+(z+z_1)^2)^2}\cdot 2y^2\right)$$

The first order term of the Taylor polynomial would vanish if the following condition applies:

$$2a^2-(z_0+z_1)^2=0 \quad \text{or} \quad z_1+z_0=a\sqrt{2}$$

Thus the field gradient is roughly constant in the plane which is $a\sqrt{2}\approx 1.41a$ far away from the plane with wires. The present apparatus has a diaphragm system in which the length of the radiation window is about $4/3a$ in the *y*-direction. As Fig. 8 shows, the value of $\partial H/\partial z$ at $y\approx 2/3a$ scarcely differs from its value at *y* = 0 (we have chosen here the plane *z* = 0 to be $1.3a$ away from the plane with wires). The condition for constant gradient is thus met to a large extent.

However we prefer technically to measure the field and not its gradient. From the relation (7) it is obvious that the gradient is proportional to the field with the coefficient ε, which depends on the space coordinates.

$$\frac{\partial H}{\partial z}=\varepsilon\cdot\frac{H}{a}$$

We repeat now the trick with the Taylor expansion of the function *ε(y,z)* in $y^2$ to find its value close to the *z*-axis (small *y*) as follows:

$$\frac{\partial H}{\partial z}= -2H(z+z_0)\cdot\frac{a^2+y^2+(z+z_0)^2}{(a^2-y^2)^2+2(z+z_0)^2\cdot(a^2+y^2)+(z+z_0)^4} \approx -\frac{2H(z+z_0)}{a^2+(z+z_0)^2}\cdot\left(1+\frac{3a^2-(z+z_0)^2}{(a^2+(z+z_0)^2)^2}\cdot y^2\right)$$

Please note that the first order term vanishes here at $3a^2-(z+z_0)^2=0$ or $z+z_0=a\sqrt{3}\approx 1.73a$ . It means that in the plane at the distance $a\sqrt{3}$ from the plane with wires the proportionality of the gradient to the field is nearly constant. (But the field as well as its gradient change across this plane, which is not the case for the $a\sqrt{2}$ one. Thus the latter plane is more practical for the experimental measurement.)

Nevertheless the last formula provides us the approximate value of the coefficient *ε* for any point in space. E.g. for the plane at $a\sqrt{2}$ ( $2a^2=(z_0+z_1)^2$ ) and *y* = 0 it will be.

$$\frac{\partial H}{\partial z}=-\frac{2H(z_1+z_0)}{a^2+(z_1+z_0)^2}=\frac{2\sqrt{2}}{3a}\cdot H=0.9428\frac{H}{a} \quad (8)$$

For the same plane but for the edge of the real extended beam $y=2/3a$ it deviates only by 5%

$$\frac{\partial H}{\partial z}=-\frac{2H(z_1+z_0)}{a^2+(z_1+z_0)^2}(1+\frac{4}{81})=\frac{2\sqrt{2}}{3a}\cdot 1.049\cdot H=0.9894\frac{H}{a}$$

The relation (8) can be then used to convert the magnetic field (measured value) into the magnetic gradient (value used in theoretical calculations) with a good approximation for the experimental beam.

The Stern-Gerlach apparatus is adjusted, so that the radiation window lies around $1.3a$ (plane *z* = 0) from the plane with imaginary wires of the two-wire system (Fig. 7).
The calibration curve of the electromagnet (magnetic field *H* against the current in coils) is likewise given for $z\approx 1.3a$ , Fig. 9. Nevertheless the coefficient of the formula (8) can still be used since this plane is very close to the one by $a\sqrt{2}$ . Otherwise the more precise value can be obtained by calculation of the *ε* as above for $z\approx 1.3a$ .

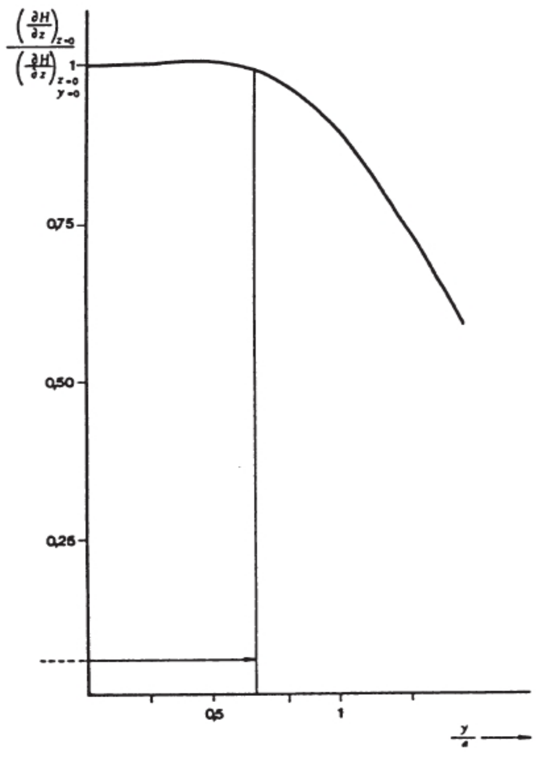


Fig. 8: Behavior the of field gradient along the radiation window.

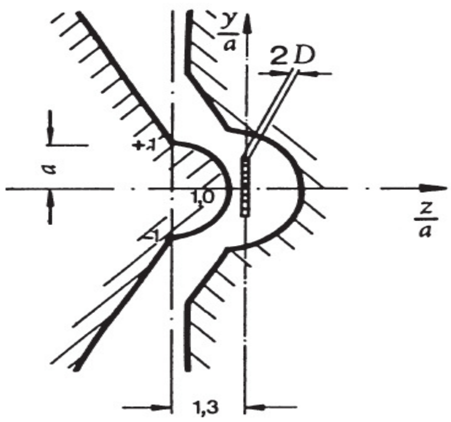


Fig. 7: Position of the atomic beam.

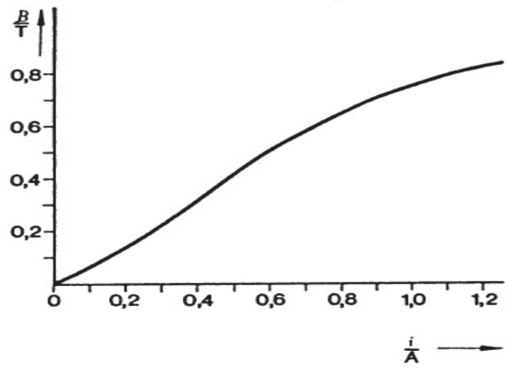


Fig. 9 : Calibration of the electromagnet, according to data sheet.

  

**4. Particle track**

The velocity *v* of all the potassium atoms entering the magnetic field can be considered with sufficient accuracy to be oriented along the x-direction. The schematic trajectory of atoms is depicted in the Fig. 10. The time

$$\Delta t = \frac{L}{v}$$

corresponds to passing through the magnetic field of the length *L* and the time

$$t = \frac{l}{v}$$

corresponds to passing from the point of entry into the magnetic field to the plane of the detector.

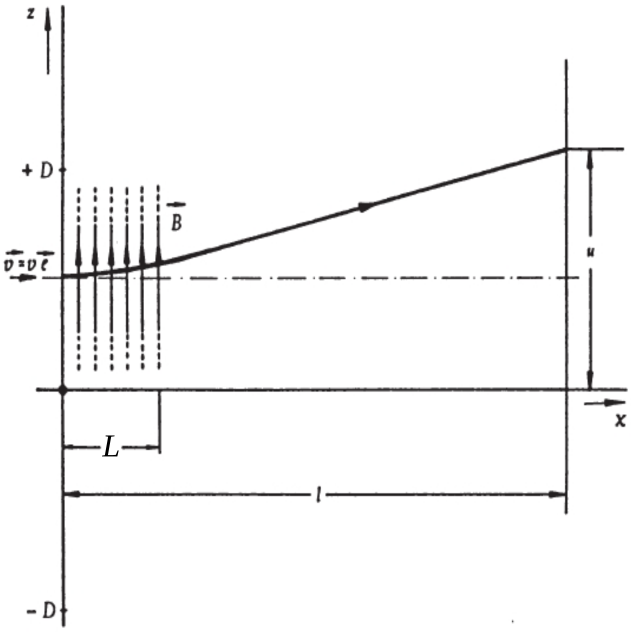


Fig. 10: Particle tracks between magnetic analyzer and detection plane.

We use the approximation of the constant force in the *z*-direction. Thus the potassium atoms of the mass *M* acquire, due to the magnetic field gradient, the following momentum along the *z*-axis

$$M\dot{z} = F_z \Delta t = F_z \frac{L}{v} = \frac{-m\mu_B L}{v} \frac{\partial B}{\partial z}$$

It follows that the point of impact *u* (in the *z*-direction) of a potassium atom with the velocity *v* in the *x*-direction and its initial position *z*, at a given field gradient, will be interconnected through the following relation:

$$u = z + \frac{1}{2}\dot{z}\,\Delta t + \dot{z}(t - \Delta t) = z + \left(1 - \frac{1}{2}\frac{L}{l}\right)\frac{l}{v}\dot{z}$$

where

$$\frac{1}{2}\dot{z}\,\Delta t$$

is the path element covered by a potassium atom during passing through the magnetic field in the *z*-direction. Hence, there is the following fundamental relationship between the deflection *u*, the particle velocity $v$ and the field gradient $\frac{\partial B}{\partial z}$

$$u = z - \frac{lL}{Mv^2}\left(1 - \frac{1}{2}\frac{L}{l}\right) m \mu_B \frac{\partial B}{\partial z} \quad (9)$$

where

$$u - z > 0 \; for \; m = +1$$
$$u - z < 0 \; for \; m = -1$$

Please notice that faster particles are deflected less into the $z$-direction than slower ones. Thus even initially an infinitesimally narrow potassium ion beam will be spread in the detector plane due to its thermal velocity distribution.

**5. Maxwell velocity distribution**

In order to produce a beam of potassium atoms of a considerable density, a furnace heated to a temperature $T$ is used. In the furnace the evaporated potassium atoms are sufficiently numerous to acquire the maxwellian velocity distribution, i.e., the probability to find an atom with a velocity between $v$ and $v + dv$ is given by the relation

$$e^{-\frac{Mv^2}{2kT}} \cdot v^2 dv$$

The current (number of particles pro time) in the detector plane for the atoms with velocities between $v + dv$ is proportional to: 1. the above-mentioned probability; 2. the velocity of arrived atoms; 3. the solid angle $d\Omega$ of the consideration (in other words to the product of these factors).

Thus the current of atoms which emerge from the opening in the furnace, and which have entered the magnetic field between $z$ and $z$ + d$z$, with a velocity between $v$ and $v$ + d$v$, will satisfy the following relation (normalized to the complete current through the analyzer):

$$d^2 n = \frac{\Phi_m(z) e^{-\frac{Mv^2}{2kT}} \cdot v^3 \, dv \, dz}{2 \int_0^\infty \mathrm{e}^{-\frac{Mv^2}{2kT}} v^3 dv} \quad (10)$$

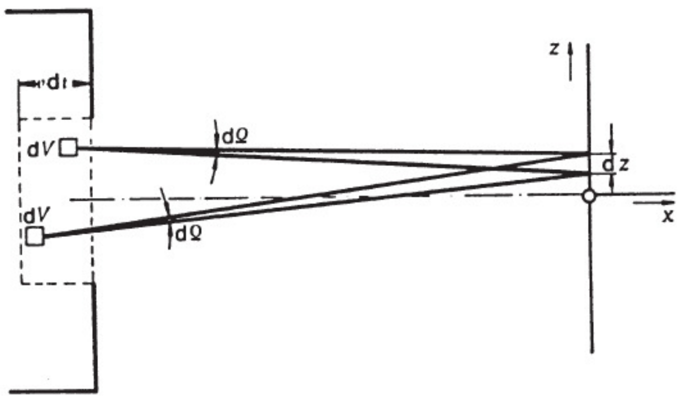


Fig. 11: Geometrical relationships for deriving the distribution function depending on $v$ and $z$.

In other words only those potassium atoms traverse the strip d*z* in time d*t* with velocity *v* at a later point in time corresponding to the transit time, which come from volume element d*V* existing in a region at depth *v*d*t* behind the opening in the furnace.

Indexing with *m* takes account of the two possible magnetic spin projections of the potassium atom. This leads to the factor of “2” in the denominator. From the symmetry it is clear that both directional orientations are equally probable. The function $\Phi_m(z)$ represents the spatial profile of the initial beam (after leaving the furnace), for particles of the spin orientation *m*. It arises through limitation of the atomic beam by appropriate systems of diaphragms. Ideally the function $\Phi_m(z)$ should resemble the Dirac delta function but in reality it has some spacial extension *D* along the z-axis (beam enclosure).

**6. Particle current density after analyzer**

Now we calculate the particle current density *I(u)* in the detector plane, as a function of the position *u*, from the distribution which depends on *v* and *z.* This will correspond to the signal at the detector. All potassium atoms entering the magnetic field at a height of *z* are spread in the detector plane according to their differences in velocity. The following conversion from *v* to *u* applies:

$$v^3\,dv=\frac{1}{4}\left(\frac{\partial v^4}{\partial u}\right)du$$

We obtain the squared velocity by the transformation of equation (9):

$$v^2=\frac{-\,lL}{M(u-z)}\left(1-\frac{1}{2}\frac{L}{l}\right)m\mu_B\frac{\partial B}{\partial z}$$

we can get rid of the magnetic projection value and use the absolute value of the shift in the magnetic field instead:

$$v^2=\frac{-\,lL}{M|u-z|}\left(1-\frac{1}{2}\frac{L}{l}\right)\mu_B\frac{\partial B}{\partial z}$$

after squaring of the last expression and differentiating the following is obtained

$$v^3\,dv=\frac{-\,1}{2}\left(\frac{lL\left(1-\frac{1}{2}\frac{L}{l}\right)\mu_B\frac{\partial B}{\partial z}}{M}\right)^2\frac{du}{|u-z|^3}$$

Furthermore,

$$\frac{Mv^2}{2kT}=\frac{-\,lL\left(1-\frac{1}{2}\frac{L}{l}\right)\mu_B\frac{\partial B}{\partial z}}{2kT}\cdot\frac{1}{|u-z|}$$

Now we introduce the two abbreviations to simplify the calculation:

$$q=\frac{-\,lL\left(1-\frac{1}{2}\frac{L}{l}\right)\mu_B\frac{\partial B}{\partial z}}{2kT}\qquad(11)$$

  

and $$n_0=\frac{\left[lL\left(1-\frac{1}{2}\frac{L}{l}\right)\mu_B\frac{\partial B}{\partial z}\right]^2}{4M^2\int_0^\infty e^{-\frac{Mv^2}{2kT}}\cdot v^3\,dv}$$

we substitute all the last expressions into and rewrite the equation (10) as following:

$$d^2n=n_0\Phi_m(z)e^{-\frac{q}{|u-z|}}\cdot\frac{du}{|u-z|^3}dz \quad (12)$$

We now integrate with respect to *z* and sum over the possible orientations *m*, and so derive the desired particle current density at position *u*:

$$I(u)=\frac{\sum_m\int_{-D}^{+D}d^2n}{du}=n_0\int_{\substack{-D\\u-z>0}}^{+D}\Phi_{+1/2}(z)e^{-\frac{q}{|u-z|}}\frac{dz}{|u-z|^3}+n_0\int_{\substack{-D\\u-z<0}}^{+D}\Phi_{-1/2}(z)e^{-\frac{q}{|u-z|}}\frac{dz}{|u-z|^3}$$

By reason of the equivalence to the particle profile of the orientations $m_s$ = –1/2 and $m_s$ = +1/2,

$$\Phi_{+1/2}(z)\equiv\Phi_{-1/2}(z)=I_0(z)$$

and hence the current will look like:

$$n_0\int_{-D}^{+D}I_0(z)e^{-\frac{q}{|u-z|}}\frac{dz}{|u-z|^3} \quad (13)$$

For a vanishing gradient of the magnetic field $u\equiv z$ and is independent of *v*. In this case, the particle current density in the measuring plane is defined as $I_0(u)$ .

**7. Infinitesimal beam cross-section**

This is the simplest (zero order) approximation which corresponds to the initially infinitely thin in the *z*-direction atomic beam which will be spread only after the magnetic field according to its velocity distribution. The beam is centered at *z* = 0. We define the initial current distribution as

$$I_0^{(0)}(z)=2DI_0\delta(z) \quad (14)$$

using the Dirac delta function $\delta$

$$\int_{-\infty}^{z_0}\delta(z)\,dz=\Theta(z_0)=\begin{cases}0\ for\ z_0<0\\1\ for\ z_0>0\end{cases}$$

For the atomic current in the detector plane we then get the integral

$$I^{(0)}(u)=2Dn_0I_0\int_{-D}^{+D}\delta(z)e^{-\frac{q}{|u-z|}}\frac{dz}{|u-z|^3}$$

using the rules of the Dirac delta function integration we easily come to the solution:

  

$$I^{(0)}(u)=2Dn_0 I_0 \frac{e^{-\frac{q}{|u|}}}{|u|^3} \quad (15)$$

The particle current density $I^{(0)}(u)$ for narrow beam profiles is therefore proportional to the width 2 *D* determined by the diaphragm system. The position $u_e$ of the intensity maximum is found by taking the first derivative and setting it equal to zero:

$$\frac{dI^0(u)}{du}=2Dn_0 I_0 \frac{q-3|u|}{u^5} e^{-\frac{q}{|u|}}$$

From the condition

$$\frac{dI^{(0)}(u)}{du}(u_e^{(0)})=0 \quad (16)$$

follows that both maxima $u_e^{(0)}$ will be symmetrical relative to zero and defined by the following expression:

$$u_e^{(0)}=\pm\frac{1}{3}q=\pm\frac{lL\left(1-\frac{1}{2}\frac{L}{l}\right)\mu_B \frac{\partial B}{\partial z}}{6kT} \quad (17)$$

The separation between the maxima (beam deflection) therefore increase proportionally to the magnetic field gradient.

## 8. Actual beam cross-section

A better compatibility of the calculation with the experiment is achieved by regarding the initial beam not infinitely narrow but extended (extension equals to 2*D*). We describe the beam profile as two steep straight lines with a parabolic apex (Fig. 12).

$$I_0(z)=i_0\begin{cases} D+z & -D\leq z\leq -p \\ D-\frac{1}{2}p-\frac{1}{2}\frac{z^2}{p} & -p\leq z\leq p \\ D-z & p\leq z\leq D \end{cases}$$

$$\frac{dI_0}{dz}=i_0\begin{cases} 1 & -D\leq z\leq -p \\ -\frac{z}{p} & -p\leq z\leq p \\ -1 & p\leq z\leq D \end{cases} \quad (18)$$

$$\frac{d^2I_0}{dz^2}=i_0\begin{cases} 0 & -D\leq z\leq -p \\ -\frac{1}{p} & -p\leq z\leq p \\ 0 & p\leq z\leq D \end{cases}$$

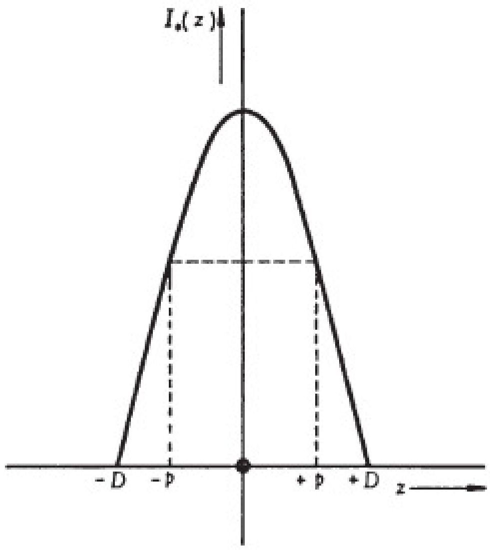


Fig. 12: Mathematical assumption of the particle current density with a vanishingly small magnetic field.

At the junction points the lines and the parabola have the same value of the first derivative. In this model, $I_0(z)$ is regarded as being twice differentiable. The particle current density $I(u)$ depends on the gradient of the magnetic field and hence on *q*. It has maxima at positions $u_e(q)$ which differ to a greater or lesser extent from the positions $u_e^{(0)}=\pm q/3$ resulting from the zero order approximation assuming an infinitesimally narrow beam.

To determine the function $u_e(q)$ we start from the condition for the extremum

$$\frac{dI}{du}(u_e)=0 \quad (19)$$

In calculating $dI/du$ , the differentiation after *u* can be incorporated within the integral

$$\frac{dI}{du}=\frac{d}{du}n_0\int_{-D}^{+D}I_0(z)\frac{e^{-\frac{q}{|u-z|}}}{|u-z|^3}dz = n_0\int_{-D}^{+D}I_0(z)\frac{\partial}{\partial u}\frac{e^{-\frac{q}{|u-z|}}}{|u-z|^3}dz$$

The integrand is not changed if $\frac{\partial}{\partial u}$ is replaced by $-\frac{\partial}{\partial z}$

$$\frac{dI}{du}=-n_0\int_{-D}^{+D}I_0(z)\frac{\partial}{\partial z}\left(\frac{e^{-\frac{q}{|u-z|}}}{|u-z|^3}\right)dz$$

The differentiation operator can be now shifted to $I_0$ using the rules of partial integration and keeping in mind that the $I_0(D) = I_0(-D) = 0$ (this will zero the additional non-integral term by partial integration).

$$\frac{dI}{du}=n_0\int_{-D}^{+D}\frac{dI_0(z)}{dz}\frac{e^{-\frac{q}{|u-z|}}}{|u-z|^3}\;dz$$

Finally we substitute the first derivative of $I_0$ into the integral and split it into four integrals, each of which can be calculated individually:

$$\frac{dI}{du}=n_0 i_0\left(\int_{-D}^{-p}\frac{e^{-\frac{q}{|u-z|}}}{|u-z|^3}dz - \frac{u}{p}\int_{-p}^{+p}\frac{e^{-\frac{q}{|u-z|}}}{|u-z|^3}dz - \int_{+p}^{+D}\frac{e^{-\frac{q}{|u-z|}}}{|u-z|^3}dz + \frac{1}{p}\int_{-p}^{+p}(u-z)\frac{e^{-\frac{q}{|u-z|}}}{|u-z|^3}dz\right)$$

The first three integrals are solved by partial integration accordingly to the scheme:
$\int e^{-\frac{q}{|t|}}\frac{1}{|t|^3}dt=\frac{q+|t|}{q^2 t}e^{-\frac{q}{|t|}}$ and the last one accordingly to $\int e^{-\frac{q}{|t|}}\frac{t}{|t|^3}dt=\frac{1}{q}e^{-\frac{q}{|t|}}$

After the integration and simplification of the expression we finally come to the following result:

$$\frac{dI}{du}=\frac{n_0 i_0}{p q^2} F(u) \quad (20)$$

with the solution function

$$F(u)= -|u+p| e^{-\frac{q}{|u+p|}} + |u-p| e^{-\frac{q}{|u-p|}} + p\frac{q+|u+D|}{u+D} e^{-\frac{q}{|u+D|}} + p\frac{q+|u-D|}{u-D} e^{-\frac{q}{|u-D|}} \quad (21)$$

As already discussed, after setting this expression equal to zero we can obtain the maxima of the current peaks in the detector plane:

$$F(u_e)=0 \quad (22)$$

The function *F(u)* is point symmetrical relative to the center of coordinates *F(-u)* = - *F(u)*. Thus also its maxima will be symmetrical relative to *u* = 0. It is therefore sufficient to restrict the evaluation to positive $u_e(q)$ .

**9. Measurement of the particle current density with a vanishingly small magnetic field**

Fig. 13 represents an example of the particle current density measured with the detector (ionization current $i_I$ in pA) as a function of the coordinate *u* in the detector plane. The magnetic field is off, the pole pieces demagnetized to get rid of the rest-magnetization. It is not necessary in this case to determine the zero point for *u.* The experimental curve is fitted by the straight lines and the parabolic segment accordingly to the previous theoretical section. The following values for *p* and *D* are obtained in the units of relative scale (turning screw of the setup) and recalculated into millimeters accordingly:

p = 0.20 scale div. = 0.36 mm
D = 0.48 scale div. = 0.86 mm.

The value for 2*D* theoretically corresponds to the width of the beam aperture before the magnetic analyzer (approximation of the parallel atomic beam). In reality the latter width is smaller due to the slight beam divergence.

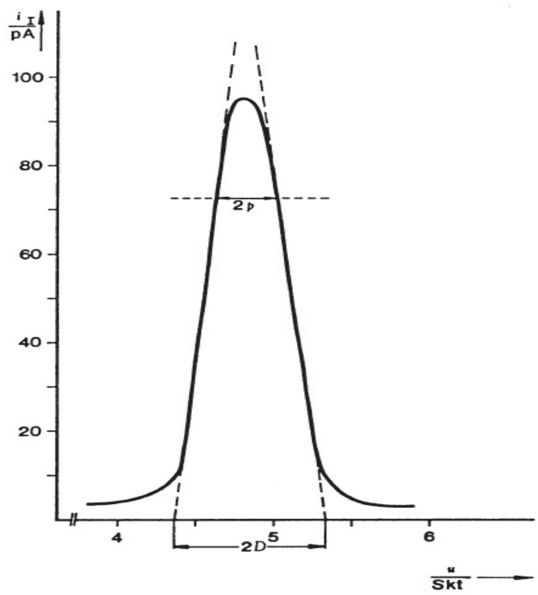


Fig. 13: Ionization current as a function of coordinate in the detector plane *u.* No magnetic field applied.

## 10. Calculation of the position of the intensity maximum

When the experimentally assigned parameters (*p*, *D*) are used, the function *F (u)* in the equation (21) gives a curve strongly dependent on *q* (Fig. 14): The points of intersection $u_e$ with the *u*-axis provide us the relation $u_e(q)$ which is depicted in the Fig. 15.

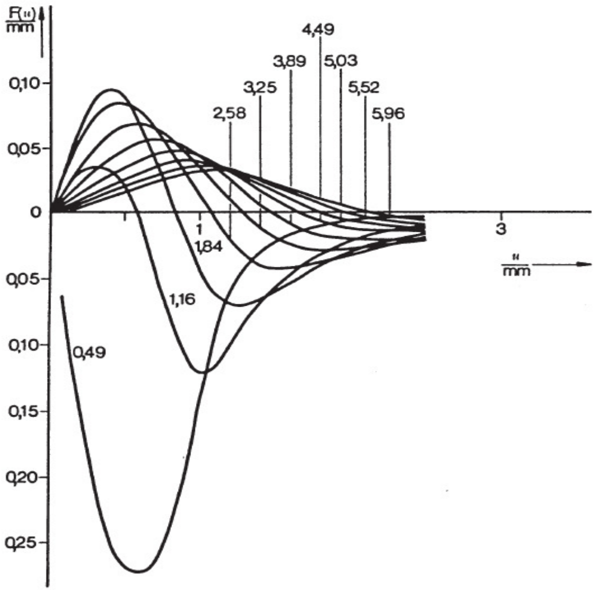


Fig. 14: Solution function *F*(*u*) for various parameters *q*. The numbers 0.49 to 5.96 correspond to *q* in mm.

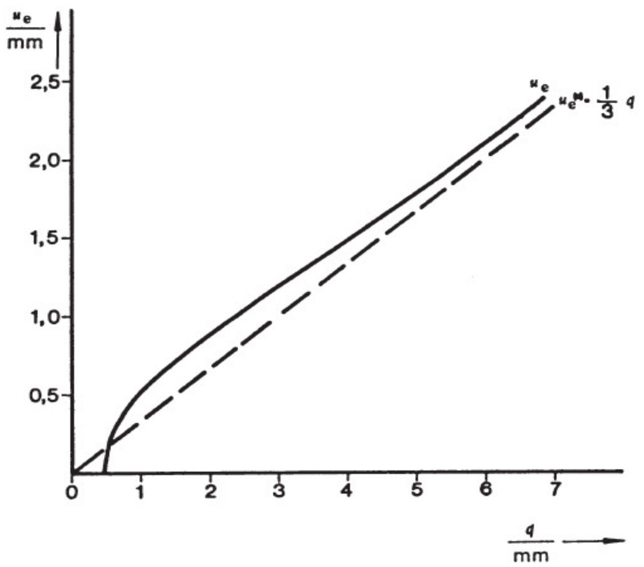


Fig. 15: Position $u_e$ of the zero point of the solution function *F*(*u*) as a function of the parameter *q*.

## 11. Calculation of the asymptotic behavior with large fields

For a sufficiently large field gradient and thus parameter *q*, $u_e$ approaches the solution given by an infinitely narrow beam. The following approximation provides the first correction for the function $u_e(q)$ for larger magnetic fieldы. Since it is assumed here that

$$u_e \sim q \gg p \sim D \quad , (23)$$

a two dimensional Taylor series for *F(u)* on the parameters *p* and *D* can be developed. The auxiliary function f(u) and its derivatives (up to the fifth one) will support the calculation.

$$f(u) = u\,e^{-\frac{q}{u}} \qquad f^{(1)}(u) = \left(1+\frac{q}{u}\right)e^{-\frac{q}{u}} \qquad f^{(2)}(u) = \frac{q^2}{u^3}e^{-\frac{q}{u}} \qquad f^{(3)}(u) = \frac{q^2}{u^4}\left(\frac{q}{u}-3\right)e^{-\frac{q}{u}}$$

$$f^{(4)}(u) = \frac{q^2}{u^5}\left(\frac{q^2}{u^2}-8\frac{q}{u}+12\right)e^{-\frac{q}{u}} \qquad f^{(5)}(u) = 12\frac{q^2}{u^6}\left(5\left(\frac{q}{u}-1\right)+\frac{1}{12}\frac{q^2}{u^2}\left(\frac{q}{u}-15\right)\right)e^{-\frac{q}{u}}$$

Now we can represent the function *F(u)* from the equation (21) with the auxiliary function *f(u)* as:

$$F(u) = -f(u+p)+f(u-p)+p\,f^{(1)}(u+D)+p\,f^{(1)}(u-D)$$

The absolute value operators were omitted due to the relations, u >0 and u >> D, p



  

The two dimensional Taylor polynomial development of the *F(u,p,D)* will be:

0th order term: $F(u,0,0)=-f(u)+f(u)+0=0$

1st $\frac{\partial F(u,0,0)}{\partial p}p+\frac{\partial F(u,o,0)}{\partial D}D=(-f^{(1)}(u)-f^{(1)}(u)+f^{(1)}(u)+f^{(1)}(u))p+(f^{(2)}(u)-f^{(2)}(u))\cdot 0\cdot D=0$

for simplicity only non zero expressions will be written down from here on

2nd order: $\frac{1}{2}\left(\frac{\partial^2 F(u,0,0)}{\partial p^2}p^2+2\frac{\partial^2 F(u,0,0)}{\partial p\,\partial D}pD+\frac{\partial^2 F(u,0,0)}{\partial D^2}D^2\right)=0$

3rd order:

$$\frac{1}{6}\left(\frac{\partial^3 F(u,0,0)}{\partial p^3}p^3+3\frac{\partial^3 F(u,0,0)}{\partial p^2\,\partial D}p^2D+3\frac{\partial^3 F(u,0,0)}{\partial p\,\partial D^2}pD^2+\frac{\partial^3 F(u,0,0)}{\partial D^3}D^3\right)=\frac{1}{6}(-2f^{(3)}(u)p^3+6f^{(3)}(u)pD^2)$$

4th order:

$$\frac{1}{24}\left(\frac{\partial^4 F}{\partial p^4}p^4+4\frac{\partial^4 F}{\partial p^3\,\partial D}p^3D+6\frac{\partial^4 F}{\partial p^2\,\partial D^2}p^2D^2+4\frac{\partial^4 F}{\partial p\,\partial D^3}pD^3+\frac{\partial^4 F}{\partial D^4}D^4\right)(u,0,0)=0$$

5th order:

$$\frac{1}{120}\left(\frac{\partial^5 F}{\partial p^5}p^5+5\frac{\partial^5 F}{\partial p^4\,\partial D}p^4D+10\frac{\partial^5 F}{\partial p^3\,\partial D^2}p^3D^2+10\frac{\partial^5 F}{\partial p^2\,\partial D^3}p^2D^3+5\frac{\partial^5 F}{\partial p\,\partial D^4}pD^4+\frac{\partial^5 F}{\partial D^5}D^5\right)(u,0,0)=\ldots$$

$$\ldots=\frac{1}{120}(-2f^{(5)}(u)p^5+5\cdot 2f^{(5)}(u)pD^4)$$

At this point we stop the Taylor polynomial development and sum the expressions above together:

$$F(u)=p\left(D^2-\frac{1}{3}p^2\right)f^{(3)}(u)+\frac{p}{12}\left(D^4-\frac{1}{5}p^4\right)f^{(5)}(u)+\ldots \quad (24)$$

To determine the maxima $u_e$ we set *F(u)* = 0 as discussed and come to the following equation:

$$0=\left(D^2-\frac{1}{3}p^2\right)\left(\frac{q}{u_e}-3\right)+\frac{D^4-\frac{1}{5}p^4}{u_e^2}\left(5\left(\frac{q}{u_e}-1\right)+\frac{1}{12}\frac{q^2}{u_e^2}\left(\frac{q}{u_e}-15\right)\right)$$

The summand on the left gives the known solution $u_e^{(0)}=\pm q/3$ if the smaller summand on the right is disregarded. When this is not done, it is permissible to replace $u_e$ by $u_e^{(0)}$ in the summand on the right to obtain the correction of the first order (on $D^4$ and $p^4$).

The quantity in parentheses on the right becomes unity:

$$0=\left(D^2-\frac{1}{3}p^2\right)\left(\frac{q}{u_e}-3\right)+\frac{D^4-\frac{1}{5}p^4}{u_e^2}$$

This equation can be rewritten as

$$q=3u_e-\frac{D^4-\frac{1}{5}p^4}{D^2-\frac{1}{3}p^2}\cdot\frac{1}{u_e} \quad (25)$$

or further to

$$u_e=\frac{q}{3}+\frac{D^4-\frac{1}{5}p^4}{D^2-\frac{1}{3}p^2}\cdot\frac{1}{q} \quad (26)$$

where we again omit the expressions of higher correction order. The formula (26) provides us the first order correction to the maxima of the atomic current.

**12. Measurements of the particle current density**

The graphs in Figs. 16 and 17 show the particle current densities (measured as ionization currents $i_I$ ) in dependence on the current in the magnetic coils and thus the field gradient. The asymmetry in height of the intensity maxima is related to the fact that the gradient of the magnetic field is slightly different on the left and the right side of the beam.

Please note that a more precise calibration curve of the electromagnet (magnetic field vs. current in coils) can be measured by the user of the Stern-Gerlach apparatus him/herself, e.g. utilizing the PHYWE Teslameter, digital, item no.: 13610-90. Otherwise the individually supplied calibration curve with each apparatus or the typical calibration curve in Fig. 9 should be used.

The field gradients at the different coil currents, according to the calibration curves of the magnet, are given in our example in the following Table:

Table

| *I*, A | $\partial B/\partial z$ , T/m |
|---|---|
| 0 | 0 |
| 0.095 | 25.6 |
| 0.200 | 58.4 |
| 0.302 | 92.9 |
| 0.405 | 132.2 |
| 0.498 | 164.2 |
| 0.600 | 196.3 |
| 0.700 | 226.0 |
| 0.800 | 253.7 |
| 0.902 | 277.2 |
| 1.010 | 298.6 |

The positions of the intensity maxima from Figs. 16 and 17 are shown in Fig. 18 as a function of the field gradient $\partial B/\partial z$

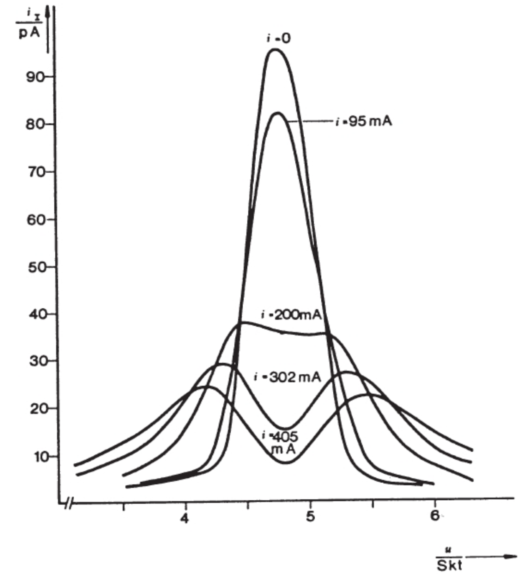


Fig. 16: Ionization current as a function of the detector position ($u$) with small currents in the magnetic coils.

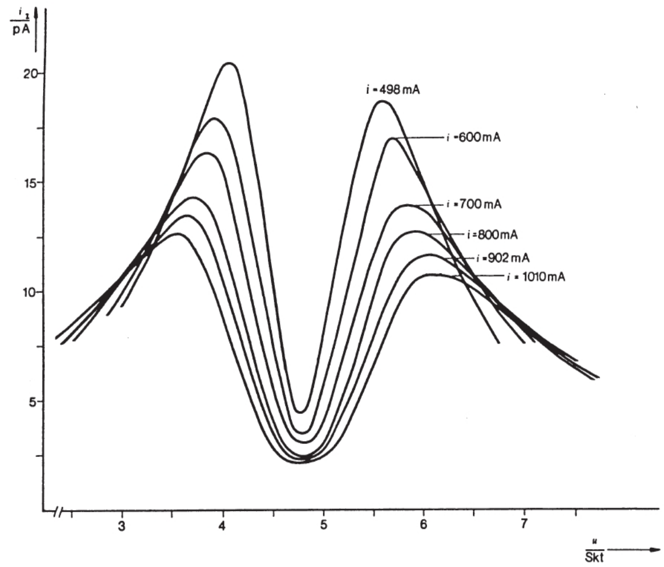


Fig. 17: Ionization current as a function of the detector position ($u$) with strong currents in the magnetic coils.

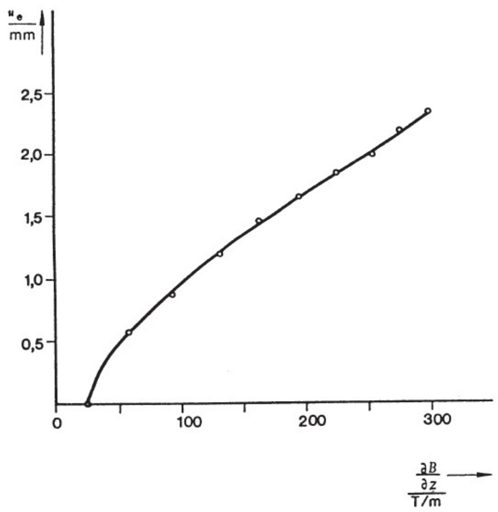


Fig. 18: Experimentally determined relationship between the position $u_e$ of the particle current maximum and the magnetic field gradient.

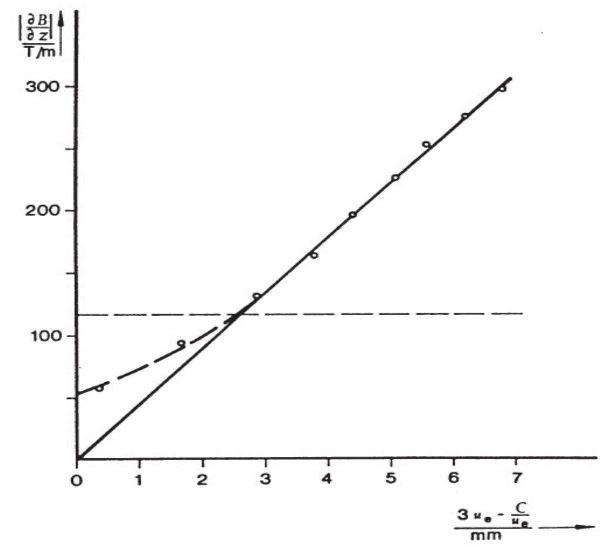


Fig. 19: Field gradient vs. a theoretical function of $u_e$ . Determination of the slope from asymptotic behavior.

## 13. Evaluation in the asymptotic limiting case

The graph in Fig. 19 shows $\partial B/\partial z$ as a function of the expression $q=3u_e-\frac{c}{u_e}$ where

$$c = \frac{D^4-\frac{1}{5}p^4}{D^2-\frac{1}{3}p^2}=0.781\,mm \quad (27)$$

  

This relation corresponds to the theoretical expression (25).

Above the horizontal broken line we fit the experimental data with the following potential function:

$$\frac{\partial B}{\partial z}=A\left(3u_e-\frac{c}{u_e}\right)^B$$

where *A* and *B* are fitting parameters. The fit results in

Potential factor: *B* = 1.00 (straight line, or linear regression)

Standard deviation: S.D.*(B)* = 0.01.

Slope: $A=44.8\frac{T/m}{mm}$

**14. Determination of the Bohr magneton**
We use the following values of the geometrical parameters of the Stern-Gerlach apparatus:

*l* = 0.455 m
*L* = 7 cm
*a* = 2.5 mm,

The absolute temperature in the furnace was
T = 453 K,

and the slope of the straight line in Fig. 19 is also known. Now we can calculate the Bohr magneton, in accordance with equations (11), (25) and (27), the value

$$\mu_B=\frac{2kT}{lL\left(1-\frac{1}{2}\frac{L}{l}\right)}\cdot\frac{3u_e-\frac{C}{u_e}}{\frac{\partial B}{\partial z}}=\frac{2kT}{lL\left(1-\frac{1}{2}\frac{L}{l}\right)A}=9.51\cdot 10^{-24}Am$$

The deviation of about 2.5% from the literature value is very small and mainly attributable to the inaccuracy of calibration of the magnetic field.

**15. Position of the intensity maxima as a function of field gradient**
From the asymptotic behavior of $u_e$ at large values of the field gradient $\partial B/\partial z$ the experiment gives, for the variable *q*:

$$\frac{q}{-\partial B/\partial z}=0.0223\cdot 10^{-3}m^2T^{-1}\quad .$$

The Fig. 20 represents the positions $u_e$ of the intensity maxima as a function of *q.* The solid line is the theory. The dashed line corresponds to the zero order theory (infinitely narrow beam). For a beam with some non zero waist the two maxima require some certain magnetic gradient to appear. Small gradient will correspond to a single central peak. As the gradient grows the two maxima appear (suddenly) to the right and left of the central axis. By higher fields the splitting is proportional to the gradient.

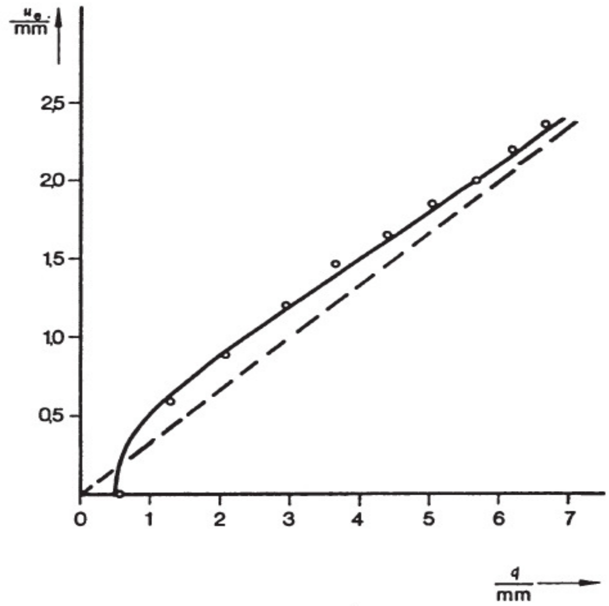


Fig. 20: Measured values for the position $u_e$ of the particle beam current maxima as a function of the variable $q$. Solid line – theory. Dashed line – theory of the zero order (infinitely narrow beam)